Received: 15 October 2018 | Revised: 13 February 2020 | Accepted: 25 May 2020

DOI: 10.1002/rnc.5105

RESEARCH ARTICLE

WILEY

Two-layer distributed formation-containment control strategy for linear swarm systems: Algorithm and experiments

Junyan Hu | **Parijat Bhowmick** | **Alexander Lanzon**

Control Systems Centre, Department of Electrical and Electronic Engineering, School of Engineering, University of Manchester, Manchester, UK

Correspondence
Parijat Bhowmick, Department of Electrical and Electronic Engineering, University of Manchester, Manchester M13 9PL, UK.
Email: Parijat.Bhowmick@manchester.ac.uk

Funding information
Engineering and Physical Sciences Research Council, Grant/Award Number: EP/R008876/1

Summary

This article addresses the problem of designing a two-layer distributed formation-containment control scheme for linear time-invariant swarm systems with directed communication topology, where the states of the leaders attain a prespecified time-varying/stationary formation and the states of the followers converge into the convex hull spanned by the states of the leaders. To achieve formation-containment, a set of distributed control protocols is developed utilizing the neighboring state information, which enables the proposed scheme operate without using global information about the entire interaction topology. The conditions to achieve formation-containment are suggested and a theoretical proof of the proposed scheme is also derived exploiting the Lyapunov stability approach. An algorithm is written to provide systematic guidelines on how to implement the control protocols in practice. It is argued that the consensus problem, formation tracking problem, and containment control problem can all be viewed as special cases of formation-containment. A simulation case study has been presented to demonstrate the usefulness and effectiveness of the proposed scheme and moreover, lab-based hardware experiments involving networked mobile robots were performed to test the feasibility of the scheme in real-time implementation.

KEYWORDS

cooperative control, formation-containment, Lyapunov stability, robotics, swarm system

1 | INTRODUCTION

In recent years, distributed cooperative control of swarm systems has drawn significant attention of numerous control engineering research communities due to its wide applications in unmanned aerial vehicles formation,[1,2] multirobots cooperation,[3] distributed energy storage systems,[4] vehicle platooning,[5] and so on. This research area includes consensus control,[6,7] rendezvous control,[8] containment control,[9,10] and formation control.[11,12] Formation control of swarm systems is therefore a key area of research, which has experienced a rapid growth over the last two decades. Pioneering research in the area of consensus-based cooperative control was done in Reference 13 which extended the first-order consensus

principles for systems with second-order dynamics and applied it in solving various formation control problems. The article[13] also argued that the existing leader-follower, behavioral and virtual leader formation control approaches can be unified in the general framework of consensus building.

Recently, with the development of algebraic graph theory, many consensus-based control strategies have been applied to deal with formation control problems.[14] Formation tracking control of first-order multiagent systems was analyzed in Reference 15. In Reference 13, a distributed formation control strategy was applied to a group of second-order swarm systems based on local neighbor-to-neighbor information exchange. A finite-time formation control protocol for second-order multiagent systems was proposed in Reference 16, where a time-invariant formation tracking is achieved within finite time. It is worth emphasizing that in some practical applications the dynamics of the agents can only be described by high-order models. Reference 17 discusses the formation stability problems for general high-order swarm systems and the result is extended to deal with formation tracking for multiple high-order autonomous agents by using a two-level consensus approach given in Reference 18. In Reference 19, adaptive group formation tracking problems was investigated but the theoretical results were not validated with real experiments. Experimental results on static formation of quadrotor swarm systems based on consensus approach were reported in Reference 20, while time-varying formation control of swarm systems is still an active area of research which requires further attention.

Another significant research topic pertaining to cooperative control of swarm systems is the containment control, which deals with multiple leaders and followers and the states of the followers are required to converge into a convex hull spanned by the states of the leaders. In Reference 21, containment control problems for both continuous-time and discrete-time multiagent systems with general linear dynamics under directed communication topologies were investigated. Containment control scheme was applied to a group of mobile autonomous agents with single-integrator kinematics under both fixed and switching communication networks in Reference 22. Besides, theoretical results for containment control of autonomous vehicles with double-integrator dynamics were validated through experiments in Reference 23. The article[24] studied the distributed containment control problem for networked Lagrangian systems with multiple dynamic leaders in presence of parametric uncertainties. However, it was assumed in Reference 24 that the leaders do not communicate among themselves, which is not usual in practical applications. In addition,[24] did not provide any experimental validation results.

Based on the formation control and containment control, the notion of formation-containment is proposed in the recent years, which requires the states of leaders to develop certain formation while the states of followers converge into the convex hull spanned by the states of the leaders. One of the potential applications of formation-containment control (FCC) is "search and rescue problem" of mobile robots in hazardous and extreme environments, where the leader robots with detection devices are able to achieve a predefined formation depending on the surrounding environment and the follower robots then move into a safe region formed by the leaders. The articles[25-27] have laid major contribution in the area of FCC of Euler-Lagrange systems: in Reference 25, a cooperative and adaptive FCC framework has been introduced for networked Euler-Lagrange systems without using relative velocity information; in Reference 26, the development of Reference 25 has been extended to consider the effect of input saturation; while in Reference 27, the FCC problem of Euler-Lagrange systems is solved in an event-triggered framework. FCC of first-order and second-order multiagent systems are investigated in References 28 and 29, respectively. LQR-based formation-containment of high-order multiagent systems is developed in Reference 30. The output formation-containment problem of coupled heterogeneous linear systems with undirected graph and directed graph are addressed in References 31 and 32, respectively. In Reference 33, the authors have proposed distributed consensus protocols to achieve leader-follower consensus in directed graphs under external disturbances. In practice, bidirectional communication is not robust and reliable when unexpected communication failure occurs. To counteract sudden communication channel disruptions during real-time implementation, it is required to study FCC with directed interaction topology. In some of the applications, a swarm system should not only accomplish the given formation-containment task, but also track the desired trajectories provided by a virtual leader, which may have nonzero control input. A virtual leader may be considered as a pseudo agent which generates the formation reference signal for the leader agents. To the best of authors' knowledge, distributed FCC problem for linear swarm systems with a virtual leader having its own control input independent of the agents and the network topology are not yet explored much.

Motivated by the issues stated above, the distributed formation-containment problem for LTI swarm systems on directed graph is investigated in this article. First, the entire swarm system is decomposed into the leaders' layer and the followers' layer and then the distributed protocols are designed based on neighboring state information which renders the controller distributed and independent of global information about the communication topology. Subsequently, the necessary conditions (known as the "formation feasibility condition") to achieve formation-containment by a swarm

system are presented which also underpin the set of feasible formations for a particular swarm system. After that, a set of distributed adaptive control protocols is designed which constitutes the FCC scheme. It is also discussed that the consensus problem, formation tracking problem and containment control problem can all be viewed as special cases of formation-containment problem solved in this article. Finally, a Matlab simulation case study is presented followed by the experimental validation results involving real robots to show the usefulness and feasibility of the proposed FCC scheme.

By contrast to the many existing FCC techniques developed so far on swarm systems, the proposed scheme of this article offers several advantages as mentioned below:

- In the present approach, we have considered a separate control input for the virtual leader (ie, the formation reference) independent of the other agents and their interactions, in contrast to the existing results on this topic which consider the virtual agent to be an autonomous system only. Due to considering the virtual leader's own control input, the time-varying formation of the leaders can also track any given bounded reference signal;
- Another advantage of the proposed scheme is that it does not need to check the eigenvalues of the graph Laplacian matrix unlike many existing cooperative control strategies on swarm systems. The proposed methodology uses only the relative state information of the agents and thereby avoids explicit computation of the Laplacian matrix which renders the scheme scalable for large-scale networked systems;
- The dynamics of the leaders and followers are not restricted to first/second-order models, which is often considered in the literature to avoid complexities. Hence this framework allows the controller design process to be carried out on the actual system dynamics of the agents. Furthermore, the communication topology among the agents can be both directed as well as undirected which enables the proposed scheme to be flexible, reconfigurable and robust to network topology changes.

Rest of the article is organized as follows. Section 2 provides the commonly used terminologies used in Graph Theory and also discusses the problem formulation. Section 3 contains the main contribution of the article, which derives a two-layer distributed FCC protocol for networked swarm systems with time-varying formation reference. An in-depth simulation case study on achieving formation-containment by a team of networked satellites is conducted in Section 4 to show the effectiveness of the proposed methodology. Section 5 provides experimental validation results involving multiple mobile robots to test the feasibility of the proposed scheme. Finally, Section 6 concludes the article mentioning the future research directions.

Notation

Notations are standard throughout. $\mathbb{R}_{>0}$ and $\mathbb{R}_{\geq 0}$ denote, respectively, the sets of all positive and all nonnegative real numbers. Let I_n denote the identity matrix of dimension $n \times n$ and $\mathbf{1}_N$ be the vector with N number of entries all being 1. $diag\{a_i\}$ represents a diagonal matrix with the diagonal entries $a_i\ \forall i$. For a real-valued function $g(t) : [0, \infty) \to \mathbb{R}^n$, $g(t) \in \mathcal{L}_2$ if $\sqrt{\int_0^\infty g(t)^T g(t)\, \mathrm{d}t} < \infty$ and $g(t) \in \mathcal{L}_\infty$ if $\sup_{t\geq 0} \|g(t)\| < \infty$. $\lambda_{\min}(X)$ denotes the minimum eigenvalue of a matrix $X \in \mathbb{R}^{n\times n}$ that has only real eigenvalues. For a real, symmetric matrix $A \geq 0, A^2$ denotes the standard matrix multiplication $A^T A = AA$; while $\sqrt{A}$ denotes the matrix square root of A such that $A = \left(\sqrt{A}\right)^2$. The Kronecker product of two matrices A and B is denoted by $A \otimes B$. $\|.\|$ expresses the 2-norm of a vector or a matrix. A square matrix $A \in \mathbb{R}^{n\times n}$ is called a nonsingular M-matrix if all its off-diagonal elements are nonpositive and all eigenvalues of A have positive real parts.[34]

2 | PRELIMINARIES AND PROBLEM FORMULATION

2.1 | Terminologies of graph theory

Consider a weighted and directed graph $\mathcal{G} = (\mathcal{V}, \mathcal{E}, \mathcal{A})$ with a nonempty set of N nodes $\mathcal{V} \in \{1, 2, \dots, N\}$, a set of edges $\mathcal{E} \subset \mathcal{V} \times \mathcal{V}$, and the associated adjacency matrix $\mathcal{A} = \left[a_{ij}\right] \in \mathbb{R}^{N\times N}$. An edge rooted at node i and ended at node j is denoted by (i, j), which means information can flow from node i to node j. a_{ij} is the weight of edge (i, j) and $a_{ij} \neq 0$ if $(i, j) \in \mathcal{E}$.

Assume that there are no repeated edges and no self-loops. Node j is called a neighbor of node i if $(i,j) \in \mathcal{E}$. Define the in-degree matrix as $D = \text{diag}\{d_i\} \in \mathbb{R}^{N\times N}$ with $d_i = \sum_{j=1}^{N} a_{ij}$. The Laplacian matrix $L \in \mathbb{R}^{N\times N}$ of $\mathcal{G}$ is defined as $L = D - \mathcal{A}$. A directed graph has or contains a directed spanning tree if there exists a node, called the root, such that the root has a directed path to every other nodes.

Lemma 1 (35). *Consider a nonsingular M-matrix L. Then there exists a diagonal matrix $G = diag\{g_1, \dots, g_N\}$ with $g_i > 0$ $\forall i \in \{1, \dots, N\}$ such that $GL + L^T G > 0$*

2.2 | Problem formulation

Consider a swarm system of N agents, which consists of M followers and rest $N - M$ leaders. Let $F = \{1, 2, \dots, M\}$ and $E = \{M + 1, M + 2, \dots, N\}$ be the sets of the followers and leaders, respectively. The dynamics of each agent is described by

$$\dot{x}_i = Ax_i + Bu_i \quad \forall i \in \{1, 2, \dots, N\}, \tag{1}$$

where $x_i = x_i(t) \in \mathbb{R}^n$ is the state of the *ith* agent and $u_i = u_i(t) \in \mathbb{R}^m$ is the associated control input for all $t \in \mathbb{R}_{\geq 0}$. $A \in \mathbb{R}^{n\times n}$ and $B \in \mathbb{R}^{n\times m}$ are constant matrices with $rank(B) = m$ and (A, B) being stabilizable. The desired trajectory of a formation (ie, the formation reference) is generated by a separate agent, called the *virtual leader*. It may be considered as the $(N + 1)th$ leader with the dynamics

$$\dot{x}_{N+1} = (A + BK_1)x_{N+1} + Bu_{N+1}, \tag{2}$$

where $x_{N+1} = x_{N+1}(t) \in \mathbb{R}^n$ and $u_{N+1} = u_{N+1}(t) \in \mathbb{R}^m$ are its state and control input, respectively, for all $t \in \mathbb{R}_{\geq 0}$ and $K_1 \in \mathbb{R}^{m\times n}$ is a constant matrix to be chosen by the designer to meet the formation feasibility condition (discussed later in Theorem 1).

Assumption 1. The bounded control input $u_{N+1}(t)$ is unknown to all leaders and followers and there exists a constant $\sigma \geq 0$ such that $\|u_{N+1}(t)\| \leq \sigma$ $\forall t \in \mathbb{R}_{\geq 0}$.

Being inspired from the developments of References 30 and 31, a two-layer framework is adopted to handle the distributed formation-containment problem, which consists of the leaders' formation layer and the followers' containment layer. In the first layer, the leaders are supposed to achieve a predetermined time-varying formation and move together following a desired reference. In the second layer, all the followers are expected to converge into a convex hull spanned by the leaders. The *two-layer formation-containment* is said to be met if and only if the control objectives in both the layers are achieved. The communication topology among each agent is denoted by $\mathcal{G}$ which satisfies the following assumption.

Assumption 2. Suppose the neighbors of a leader are only leaders or the virtual leader, and the neighbors of a follower are either leaders or followers.

Under Assumption 2, the Laplacian matrix L associated with the graph $\mathcal{G}$ can be partitioned as

$$L = \begin{bmatrix} L_1 & L_2 & 0_{M\times 1} \\ 0_{(N-M)\times M} & L_3 & L_4 \\ 0_{1\times M} & 0_{1\times(N-M)} & 0_{1\times 1} \end{bmatrix}, \tag{3}$$

where $L_1 \in \mathbb{R}^{M\times M}$, $L_2 \in \mathbb{R}^{M\times(N-M)}$, $L_3 \in \mathbb{R}^{(N-M)\times(N-M)}$, and $L_4 \in \mathbb{R}^{(N-M)\times 1}$. Desired formation of the leaders is specified by the vector $h_E = \left[h_{M+1}^T, h_{M+2}^T, \dots, h_N^T\right]^T$ where $h_i \in \mathbb{R}^n$ for all $i \in E$. h_i can be time-varying as well and in that case, $h_i(t) \in \mathbb{R}^n$ for all $t \in \mathbb{R}_{\geq 0}$. Desired formation h_i is prespecified to the *ith* leader. For simplicity of presentation, explicit dependence of h_i on time $t \in \mathbb{R}_{\geq 0}$ is omitted.

Definition 1. The leaders are said to achieve time-varying formation tracking with the virtual leader if for any given bounded initial states and any $j \in E$,

$$\lim_{t\to\infty} \left(x_j(t) - h_j(t) - x_{N+1}(t)\right) = 0. \tag{4}$$

Definition 2. The followers are said to achieve containment if for any given bounded initial states and any $k \in F$, there exist nonnegative constants α_{kj} satisfying $\sum_{j=M+1}^{N} \alpha_{kj} = 1$ such that

$$\lim_{t\to\infty}\left(x_k(t) - \sum_{j=M+1}^{N} \alpha_{kj} x_j(t)\right) = 0. \tag{5}$$

Definition 3. The swarm system (1) is said to achieve formation-containment if for any given bounded initial states, any $k \in F$ and $j \in E$, there exist nonnegative constants α_{kj} satisfying $\sum_{j=M+1}^{N} \alpha_{kj} = 1$ such that (4) and (5) hold simultaneously.

Remark 1. According to Definitions 1 to 3, it can be argued that if $M = 0$, the two-layer formation-containment problem reduces to "formation tracking" problem. If $M = 0$ and $h_E \equiv 0$, the formation-containment problem specializes to "consensus seeking" problem. Moreover, if $h_E \equiv 0$ and leaders have no neighbors, then we can conclude that the formation-containment problem specializes to "containment" problem. Therefore, the consensus seeking, formation tracking and containment control can all be viewed as special cases of FCC problem.

In this article, we introduce a distributed time-varying FCC protocol given below:

$$\begin{cases} u_i = K_1 x_i + (c_i + \rho_i) K_2 \xi_i - \mu f(\xi_i) \\ \dot{c}_i = \xi_i^T \Gamma \xi_i \end{cases} \qquad \forall i \in E; \tag{6}$$

$$\begin{cases} u_i = K_1 x_i + (\hat{c}_i + \hat{\rho}_i) K_2 \varsigma_i - \eta f(\varsigma_i) \\ \dot{\hat{c}}_i = \varsigma_i^T \Gamma \varsigma_i \end{cases} \qquad \forall i \in F; \tag{7}$$

where

$$\xi_i = \sum_{j=M+1}^{N} a_{ij}\left[(x_i - h_i) - (x_j - h_j)\right] + a_{i,N+1}\left[(x_i - h_i) - x_{N+1}\right] \quad \text{and} \quad \varsigma_i = \sum_{j=1}^{N} a_{ij}(x_i - x_j). \tag{8}$$

Above, $c_i(t)$ and $\hat{c}_i(t)$ denote the time-varying coupling weights associated with the *ith* agent with $c_i(0) \geq 0$ and $\hat{c}_i(0) \geq 0$; $K_1 \in \mathbb{R}^{m\times n}$, $K_2 \in \mathbb{R}^{m\times n}$ and $\Gamma \in \mathbb{R}^{n\times n}$ are constant matrices to be chosen; η and μ are positive constants to be selected; $\hat{\rho}_i$ and ρ_i are smooth functions of ς_i and ξ_i, respectively; and $f(.)$ represents a nonlinear function to be determined later.

If two-layer formation-containment is achieved, the leaders will first attain the desired formation (time-varying/stationary) and keep tracking the reference trajectory generated by the virtual leader, and after that, the followers will converge into the convex hull spanned by the leaders. This article primarily focuses on the following issues: (i) under which conditions the formation-containment can be achieved, and (ii) the steps to design a distributed (ie, distributed and adaptive) control protocol to achieve two-layer formation-containment.

3 | FCC PROTOCOL DESIGN

In this section, the problem of designing a distributed FCC protocol for LTI swarm systems, represented by (1), is investigated.

Assumption 3. The interaction topology among the leaders has a spanning tree with the virtual leader being the root node.

Assumption 4. For each follower, there exists at least one leader that has a directed path to it.

The following lemma taken from Reference 36 can be proved under Assumptions 3 and 4.

Lemma 2 (36). *If the directed interaction topology $\mathcal{G}$ satisfies Assumptions 3 and 4, then all the eigenvalues of L_1 and L_3 have positive real parts, each entry of $-L_1^{-1}L_2$ is nonnegative, and each row of $-L_1^{-1}L_2$ has a sum equal to one.*

Let $x_F = \left[x_1^T, x_2^T, \dots, x_M^T\right]^T$, $x_E = \left[x_{M+1}^T, x_{M+2}^T, \dots, x_N^T\right]^T$, $F(\varsigma) = \left[f^T(\varsigma_1), f^T(\varsigma_2), \dots, f^T(\varsigma_M)\right]^T$ and $F(\xi) = \left[f^T(\xi_{M+1}), f^T(\xi_{M+2}), \dots, f^T(\xi_N)\right]^T$. Note that x_F and x_E are variables of time $t \in \mathbb{R}_{\geq 0}$. Applying the distributed FCC protocols

(7) and (6), the closed-loop dynamics of the swarm system (1) can be written in a compact form as

$$\begin{cases} \dot{x}_E = [I_{N-M} \otimes (A + BK_1) + (C + \rho)L_3 \otimes BK_2]\, x_E + [(C + \rho)L_4 \otimes BK_2]\, x_{N+1} - [(C + \rho)L_3 \otimes BK_2]\, h_E \\ \qquad -\mu(I_{N-M} \otimes B)F(\xi) \\ \dot{c}_i = \xi_i^T \Gamma \xi_i; \end{cases} \tag{9}$$

$$\begin{cases} \dot{x}_F = \left[I_M \otimes (A + BK_1) + (\hat{C} + \hat{\rho})L_1 \otimes BK_2\right] x_F + \left[(\hat{C} + \hat{\rho})L_2 \otimes BK_2\right] x_E - \eta(I_M \otimes B)F(\varsigma) \\ \dot{\hat{c}}_i = \varsigma_i^T \Gamma \varsigma_i; \end{cases} \tag{10}$$

where $\hat{C} = diag\{\hat{c}_1, \dots, \hat{c}_M\}$, $\hat{\rho} = diag\{\hat{\rho}_1, \dots, \hat{\rho}_M\}$, $C = diag\{c_{M+1}, \dots, c_N\}$, and $\rho = diag\{\rho_{M+1}, \dots, \rho_N\}$.

Let the global formation tracking error vector of the leaders be $\xi = [\xi_{M+1}^T, \dots, \xi_N^T]^T$ where ξ_i for all $i \in \{M+1, \dots, N\}$ are as defined in (8). Let $z_i = x_i - h_i$ for all $i \in E$ and $z_E = \left[z_{M+1}^T, \dots, z_N^T\right]^T$. Now ξ can be written in the Kronecker product form as

$$\xi = (L_3 \otimes I_n)z_E + (L_4 \otimes I_n)x_{N+1}. \tag{11}$$

If formation tracking is achieved asymptotically by the leaders, then we have $\lim_{t\to\infty}\xi(t) = 0$ which implies from (11)

$$\lim_{t\to\infty} \left[x_E(t) - h_E(t) + L_3^{-1}L_4 \otimes x_{N+1}(t)\right] = 0. \tag{12}$$

From Assumption 3, it follows that $L_3^{-1}L_4 = -\mathbf{1}_{N-M}$ and plugging this in (12) yields

$$\lim_{t\to\infty} \left[x_E(t) - h_E(t) - \mathbf{1}_{N-M} \otimes x_{N+1}(t)\right] = 0. \tag{13}$$

Subsequently, the global containment error vector of the followers, denoted by $\varsigma = [\varsigma_1^T, \dots, \varsigma_M^T]^T$, is expressed in a compact form as

$$\varsigma = (L_2 \otimes I_n)x_E + (L_1 \otimes I_n)x_F. \tag{14}$$

Note that x_E, x_F and ξ are all time-dependent vectors. If the containment phase is reached asymptotically by the followers, then we can write $\lim_{t\to\infty} \varsigma(t) = 0$. This implies from (14)

$$\lim_{t\to\infty} \left[x_F(t) - (-L_1^{-1}L_2 \otimes I_n)x_E(t)\right] = 0. \tag{15}$$

Therefore, the swarm system (1) achieves the formation-containment by applying the distributed FCC protocol (7) and (6), if for any given bounded initial states,

$$\begin{cases} \lim_{t\to\infty} \varsigma(t) = 0 \quad \text{and} \\ \lim_{t\to\infty} \xi(t) = 0. \end{cases} \tag{16}$$

The following theorem is the main contribution of this article which establishes the conditions to be satisfied by the swarm systems (1) to achieve formation-containment applying the distributed FCC protocol proposed in (7) and (6), provided the agents and the network hold certain properties. Moreover, the virtual leader has its own control input u_{N+1} independent of the dynamics of the agents and the network topology.

Theorem 1. *Suppose, Assumptions 1 to 4 hold and for a given $\sigma \geq 0$, the constants η and μ satisfy the relation*

$$\eta \geq \mu \geq \sigma. \tag{17}$$

If the following formation feasibility condition

$$(A + BK_1)(h_i - h_j) - (\dot{h}_i - \dot{h}_j) = 0 \quad \forall i, j \in E \tag{18}$$

is satisfied for a given choice of $K_1 \in \mathbb{R}^{m\times n}$ *and* $h_i(t) \in \mathbb{R}^n\ \forall t \in \mathbb{R}_{\geq 0}$, *then the two-layer formation-containment is achieved by the distributed FCC protocol given in (6) and (7) with* $K_2 = -R^{-1}B^TP$, $\Gamma = PBR^{-1}B^TP$, $\hat{\rho}_i = \varsigma_i^T P \varsigma_i$ *and* $\rho_i = \xi_i^T P \xi_i$ *where* $P > 0$ *is the solution of the algebraic Riccati equation*

$$(A + BK_1)^T P + P(A + BK_1) + Q - PBR^{-1}B^TP = 0 \tag{19}$$

for given $Q > 0$ *and* $R > 0$. *The nonlinear function* $f(.)$ *used in (7) and (6) is designed as:*

$$f(\chi) = \begin{cases} \frac{B^TP\chi}{\|B^TP\chi\|} & \text{when } \|B^TP\chi\| \neq 0 \\ 0 & \text{when } \|B^TP\chi\| = 0, \end{cases} \tag{20}$$

where $\chi \in \mathbb{R}^n$ *represents either* ς_i *or* ξ_i *for all* $i \in \{1, 2, \dots, N\}$.

Proof. The proof has been divided into two parts: Part I establishes the formation tracking by the leaders; while Part II deals with containment of the followers.

(**Part I:** *Formation tracking*) We first derive the closed-loop dynamics of the leaders approaching formation tracking with the help of the proposed distributed and adaptive control law (6). Substituting (6) into (1) and then, substituting further the resulting expression into the derivative of (11), we obtain

$$\begin{cases} \dot{\xi} = [I_{N-M} \otimes (A + BK_1) + (C + \rho)L_3 \otimes BK_2]\,\xi + [L_3 \otimes (A + BK_1)]h_E - (L_3 \otimes I_n)\dot{h}_E - \mu(L_3 \otimes B)F(\xi) \\ \qquad -(L_3\mathbf{1}_{N-M} \otimes B)u_{N+1} \quad \text{and} \\ \dot{c}_i = \xi_i^T \Gamma \xi_i. \end{cases} \tag{21}$$

Achieving formation tracking by the leaders is posed as an asymptotic stability problem of the closed-loop dynamics (21) involving $\dot{\xi}$ and $\dot{c}_i$. In order to prove asymptotic stability of (21) using Lyapunov stability approach, we consider the following Lyapunov function candidate

$$V_1 = \frac{1}{2}\sum_{i=M+1}^{N} g_i(2c_i + \rho_i)\rho_i + \frac{1}{2}\sum_{i=M+1}^{N} g_i(c_i - \alpha)^2, \tag{22}$$

where $g_i > 0$ for all i, $c_i(t) > 0$ for all $t \geq 0$ and for all i since $\Gamma > 0$, $\rho_i > 0$ for all i since $P > 0$, and $\alpha > 0$. Therefore, $V_1 > 0$. Since the sub-Laplacian matrix L_3 corresponding to the interaction topology of the leaders is a nonsingular M-matrix (exploiting the property given in Lemma 2), there exists a diagonal positive definite matrix $G \in \mathbb{R}^{(N-M)\times(N-M)}$ such that

$$GL_3 + L_3^T G > 0 \tag{23}$$

holds via Lemma 1. As the scalar parameters g_i can take any positive values as decided by the designer, we may choose $G = diag\{g_{M+1}, g_{M+2}, \dots, g_N\}$ such that (23) is satisfied. The time derivative of V_1 along any trajectories of (21) is obtained as:

$$\begin{aligned} \dot{V}_1 &= \sum_{i=M+1}^{N} \left[g_i(c_i + \rho_i)\dot{\rho}_i + g_i\rho_i\dot{c}_i\right] + \sum_{i=M+1}^{N} g_i(c_i - \alpha)\dot{c}_i \\ &= \sum_{i=M+1}^{N} 2g_i(c_i + \rho_i)\xi_i^T P\dot{\xi}_i + \sum_{i=M+1}^{N} g_i(\rho_i + c_i - \alpha)\dot{c}_i. \end{aligned} \tag{24}$$

We will first convert the summation terms present in (24) into the Kronecker product form aiming to finally express $\dot{V}_1$ in a quadratic form with respect to ξ. Note that

$$\sum_{i=M+1}^{N} g_i(\rho_i + c_i - \alpha)\dot{c}_i = \xi^T\left[(C + \rho - \alpha I)\,G \otimes \Gamma\right]\xi, \tag{25}$$

and

$$\begin{aligned}
&\sum_{i=M+1}^{N} 2g_i(c_i+\rho_i)\xi_i^T P\dot{\xi}_i \\
&= 2\,\xi^T\left[(C+\rho)G\otimes P\right]\dot{\xi} \\
&= \xi^T\left[(C+\rho)G\otimes\left[P(A+BK_1)+(A+BK_1)^TP\right]-(C+\rho)(GL_3+L_3^TG)(C+\rho)\otimes\Gamma\right]\xi \\
&\quad + 2\xi^T[(C+\rho)GL_3\otimes P(A+BK_1)]h_E - 2\xi^T\left[(C+\rho)GL_3\otimes P\right]\dot{h}_E - 2\mu\xi\left[(C+\rho)GL_3\otimes PB\right]F(\xi) \\
&\quad - 2\xi\left[(C+\rho)GL_3\otimes PB\right](\mathbf{1}_{N-M}\otimes u_{N+1}) \\
&\le \xi^T\left[(C+\rho)G\otimes[P(A+BK_1)+(A+BK_1)^TP]-\lambda_0^{\min}(C+\rho)^2\otimes\Gamma\right]\xi \\
&\quad + 2\,\xi^T\left[(C+\rho)GL_3\otimes P(A+BK_1)\right]h_E - 2\xi^T\left[(C+\rho)GL_3\otimes P\right]\dot{h}_E - 2\mu\xi^T\left[(C+\rho)GL_3\otimes PB\right]F(\xi) \\
&\quad - 2\,\xi\left[(C+\rho)GL_3\otimes PB\right](\mathbf{1}_{N-M}\otimes u_{N+1})
\end{aligned} \tag{26}$$

where $\lambda_0^{\min}$ represents the smallest positive eigenvalue of $\left[GL_3+L_3^TG\right]$. We will now simplify each of the terms appearing in expressions (25) and (26). From (20), it is straightforward to show that

$$\xi_i^T PBf(\xi_i) = \left\|B^TP\xi_i\right\| \quad \forall i\in\{M+1,M+2,\dots,N\}. \tag{27}$$

Applying Cauchy-Schwarz inequality[37] on (27), we obtain

$$\begin{aligned}
\xi_i^T PBf(\xi_j) &\le \left\|B^TP\xi_i\right\|\left\|f(\xi_j)\right\| \\
&= \left\|B^TP\xi_i\right\| \quad \forall i\ne j.
\end{aligned} \tag{28}$$

We now simplify the following term containing $F(\xi)$

$$\begin{aligned}
&-2\mu\,\xi^T\left[(C+\rho)GL_3\otimes PB\right]F(\xi) \\
&= -2\mu\sum_{i=M+1}^{N}(c_i+\rho_i)g_i\xi_i^TPB\sum_{j=M+1}^{N}a_{ij}[f(\xi_i)-f(\xi_j)] - 2\mu\sum_{i=M+1}^{N}(c_i+\rho_i)g_ia_{i,N+1}\xi_i^TPBf(\xi_i) \\
&= -2\mu\sum_{i=M+1}^{N}(c_i+\rho_i)g_i\sum_{j=M+1}^{N}a_{ij}\left[\xi_i^TPBf(\xi_i)-\xi_i^TPBf(\xi_j)\right] - 2\mu\sum_{i=M+1}^{N}(c_i+\rho_i)g_ia_{i,N+1}\xi_i^TPBf(\xi_i) \\
&\le -2\mu\sum_{i=M+1}^{N}(c_i+\rho_i)g_ia_{i,N+1}\left\|B^TP\xi_i\right\|
\end{aligned} \tag{29}$$

since $\left[\xi_i^TPBf(\xi_i)-\xi_i^TPBf(\xi_j)\right]\le 0\ \forall i$ from (27) and (28), and rest of the parameters c_i, ρ_i, g_i, μ are all positive. Subsequently, we simplify another component, as shown below, involving the virtual leader's input u_{N+1}

$$\begin{aligned}
&-2\,\xi\left[(C+\rho)GL_3\otimes PB\right](\mathbf{1}_{N-M}\otimes u_{N+1}) \\
&= -2\sum_{i=M+1}^{N}(c_i+\rho_i)g_ia_{i,N+1}\xi_i^TPBu_{N+1} \\
&\le 2\sum_{i=M+1}^{N}(c_i+\rho_i)g_ia_{i,N+1}\left\|B^TP\xi_i\right\|\|u_{N+1}\| \\
&\le 2\,\sigma\sum_{i=M+1}^{N}(c_i+\rho_i)g_ia_{i,N+1}\left\|B^TP\xi_i\right\| \quad \text{[due to Assumption 2].}
\end{aligned} \tag{30}$$

Applying the simplified conditions (29) and (30) into (26) and selecting $\mu\ge\sigma$, the expression for $\dot{V}_1$ reduces to

$$\dot{V}_1 \le\ \xi^T[(C+\rho)G\otimes[P(A+BK_1)+(A+BK_1)^TP+\Gamma]-(\lambda_0^{\min}(C+\rho)^2+\alpha G)\otimes\Gamma]\xi$$

$$+ 2\xi^T[(C+\rho)GL_3 \otimes P(A+BK_1)]h_E - 2\xi^T[(C+\rho)GL_3 \otimes P]\dot{h}_E - 2(\mu-\sigma)\sum_{i=M+1}^{N}(c_i+\rho_i)g_i a_{i,N+1}\left\|B^T P\xi_i\right\|$$
$$\leq \xi^T[(C+\rho)G \otimes [P(A+BK_1) + (A+BK_1)^T P + \Gamma] - (\lambda_0^{\min}(C+\rho)^2 + \alpha G) \otimes \Gamma]\xi$$
$$+ 2\xi^T[(C+\rho)GL_3 \otimes P(A+BK_1)]h_E - 2\xi^T[(C+\rho)GL_3 \otimes P]\dot{h}_E. \tag{31}$$

Now, the formation feasibility condition (18) can be expressed in a compact form

$$[L_3 \otimes (A+BK_1)]h_E - (L_3 \otimes I_n)\dot{h}_E = 0, \tag{32}$$

and upon premultiplying both sides of (32) by $(C+\rho)G \otimes P$, we get

$$[(C+\rho)GL_3 \otimes P(A+BK_1)]h_E - [(C+\rho)GL_3 \otimes P]\dot{h}_E = 0. \tag{33}$$

Plugging (33) into (31), the expression of $\dot{V}_1$ further reduces to

$$\dot{V}_1 \leq \xi^T\left[(C+\rho)G \otimes [P(A+BK_1) + (A+BK_1)^T P + \Gamma] - (\lambda_0^{\min}(C+\rho)^2 + \alpha G) \otimes \Gamma\right]\xi. \tag{34}$$

Now using a common matrix property $X^2 + Y^2 \geq 2XY$ where $X > 0$, $Y > 0$,[38] we simplify the term $\left[\lambda_0^{\min}(C+\rho)^2 + \alpha G\right] \otimes \Gamma$ as follows

$$-\xi^T\left[(\lambda_0^{\min}(C+\rho)^2 + \alpha G) \otimes \Gamma\right]\xi \leq -2\xi^T\left[\sqrt{\lambda_0^{\min}\ \alpha(C+\rho)^2\ G} \otimes \Gamma\right]\xi \tag{35}$$

assuming $X = \sqrt{\lambda_0^{\min}}\,(C+\rho) > 0$ and $Y = \sqrt{\alpha\ G} > 0$. Selecting $\alpha \geq \frac{max_{i\in E} g_i}{\lambda_0^{\min}}$, $\mu \geq \sigma$ and substituting (35) into (34), the expression of $\dot{V}_1$ becomes

$$\dot{V}_1 \leq \xi^T\left[(C+\rho)G \otimes \left(P(A+BK_1) + (A+BK_1)^T P - \Gamma\right)\right]\xi. \tag{36}$$

Let us introduce a change of variable $\zeta = \left(\sqrt{(C+\rho)G} \otimes I\right)\xi$ in (36) and it yields

$$\dot{V}_1 \leq \zeta^T\left[I_{N-M} \otimes \left(P(A+BK_1) + (A+BK_1)^T P - PBR^{-1}B^T P\right)\right]\zeta. \tag{37}$$

This implies $\dot{V}_1 \leq 0$ using the ARE given in (19), and $\dot{V}_1 = 0$ when $\zeta = 0$. Therefore, by applying the LaSalle's invariance principle,[37] the closed-loop dynamics (21) can be guaranteed to be asymptotically stable. It ensures

$$\lim_{t\to\infty}\zeta(t) = 0 \tag{38}$$

which in turn ensures

$$\lim_{t\to\infty}\xi(t) = 0 \tag{39}$$

since ζ and ξ are related via nonsingular transformation. The result (39) confirms that the leaders asymptotically achieve the prespecified formation given by h_E under the influence of the proposed formation tracking control law (6) while keep tracking the reference (x_{N+1}) provided by the virtual leader.

(**Part II:** *Containment*) Once the leaders achieve time-varying formation tracking under the application of the proposed formation tracking protocol (6), it is now the turn of the followers to undergo the containment phase. We will start with deriving the closed-loop containment error dynamics $(\dot{\varsigma})$ of the followers. Inserting the containment control law (7) into (10) and invoking (11)-(14), we obtain the dynamics of $\dot{\varsigma}$ and $\dot{\hat{c}}_i$ as mentioned below:

$$\begin{cases}\dot{\varsigma} = \left[I_M \otimes (A+BK_1) + (\hat{C}+\hat{\rho})L_1 \otimes BK_2\right]\varsigma + [(C+\rho)L_2L_3 \otimes BK_2]\left[x_E(t) - h_E(t) - \mathbf{1}_{N-M} \otimes x_{N+1}(t)\right] \\ \qquad -\eta(L_1 \otimes B)F(\varsigma) - \mu(L_2 \otimes B)F(\xi) \quad \text{and} \\ \dot{\hat{c}}_i = \varsigma_i^T\Gamma\varsigma_i.\end{cases} \tag{40}$$

Similar to Part I, achieving containment by the followers has been cast as an asymptotic stability problem of the containment error dynamics (40). Following the Lyapunov approach adopted in Part I to establish asymptotic stability, in Part II also, we consider a similar Lyapunov function candidate

$$V_2 = \frac{1}{2}\sum_{i=1}^{M}\varphi_i(2\hat{c}_i + \hat{\rho}_i)\hat{\rho}_i + \frac{1}{2}\sum_{i=1}^{M}\varphi_i(\hat{c}_i - \beta)^2 \tag{41}$$

which consists of $\varphi_i > 0$ for all $i \in \{1, \dots, M\}$, $\hat{c}_i(t) > 0$ for all $t \geq 0$ and for all i since $\Gamma > 0$, $\hat{\rho}_i > 0$ for all i since $P > 0$, and $\beta > 0$. Thus, $V_2 > 0$. Since the sub-Laplacian matrix L_1 corresponding to the leaders' interaction graph is a nonsingular M-matrix according to Lemma 2, there exists a diagonal positive definite matrix $\Xi \in \mathbb{R}^{M\times M}$ such that

$$\Xi L_1 + L_1^T\Xi > 0 \tag{42}$$

holds via Lemma 1. As the scalar parameters φ_i can take any positive values, we may propose $\Xi = diag\{\varphi_1, \varphi_2, \dots, \varphi_M\} > 0$ such that (42) is satisfied. The next step is to find $\dot{V}_2$ along the trajectory of (40) as shown below:

$$\begin{aligned}\dot{V}_2 &= \sum_{i=1}^{M}\left[\varphi_i(\hat{c}_i + \hat{\rho}_i)\dot{\hat{\rho}}_i + \varphi_i\hat{\rho}_i\dot{\hat{c}}_i\right] + \sum_{i=1}^{M}\varphi_i(\hat{c}_i - \beta)\dot{\hat{c}}_i \\ &= \sum_{i=1}^{M}2\varphi_i(\hat{c}_i + \hat{\rho}_i)\varsigma_i^T P\dot{\varsigma}_i + \sum_{i=1}^{M}\varphi_i(\hat{\rho}_i + \hat{c}_i - \beta)\dot{\hat{c}}_i.\end{aligned} \tag{43}$$

Similar to Part I, $\dot{V}_2$ needs to be expressed in a quadratic form with respect to ς. In order to do so, we expand the summation-terms present in (43) and rearrange them in the Kronecker product form:

$$\sum_{i=1}^{M}\varphi_i(\hat{\rho}_i + \hat{c}_i - \beta)\dot{\hat{c}}_i = \varsigma^T\left[(\hat{C} + \hat{\rho} - \beta I)\Xi \otimes \Gamma\right]\varsigma \tag{44}$$

and

$$\begin{aligned}\sum_{i=1}^{M}2\varphi_i(\hat{c}_i + \hat{\rho}_i)\varsigma_i^T P\dot{\varsigma}_i &= 2\,\varsigma^T\left[(\hat{C} + \hat{\rho})\Xi \otimes P\right]\dot{\varsigma} \\ &= \varsigma^T\left[(\hat{C} + \hat{\rho})\Xi \otimes \left(P(A + BK_1) + (A + BK_1)^T P\right) - (\hat{C} + \hat{\rho})(\Xi L_1 + L_1^T\Xi)(\hat{C} + \hat{\rho}) \otimes \Gamma\right]\varsigma \\ &\quad + 2\,\varsigma^T\left((C + \rho)\Xi L_2 L_3 \otimes PBK_2\right)(x_E - h_E - \mathbf{1}_{N-M} \otimes x_{N+1}) - 2\eta\varsigma^T\left[(\hat{C} + \hat{\rho})\Xi L_1 \otimes PB\right]F(\varsigma) \\ &\quad - 2\,\mu\,\varsigma^T\left[(\hat{C} + \hat{\rho})\Xi L_2 \otimes PB\right]F(\xi) \\ &\leq \varsigma^T\left[(\hat{C} + \hat{\rho})\Xi \otimes \left(P(A + BK_1) + (A + BK_1)^T P\right) - \lambda_1^{\min}(\hat{C} + \hat{\rho})^2 \otimes \Gamma\right]\varsigma \\ &\quad + 2\,\varsigma^T\left((C + \rho)\Xi L_2 L_3 \otimes PBK_2\right)(x_E - h_E - \mathbf{1}_{N-M} \otimes x_{N+1}) - 2\eta\varsigma^T\left[(\hat{C} + \hat{\rho})\Xi L_1 \otimes PB\right]F(\varsigma) \\ &\quad - 2\,\mu\,\varsigma^T\left[(\hat{C} + \hat{\rho})\Xi L_2 \otimes PB\right]F(\xi),\end{aligned} \tag{45}$$

where $\lambda_1^{\min}$ represents the smallest positive eigenvalue of $\left[\Xi L_1 + L_1^T\Xi\right]$. We will now simplify the components of (45) which are not in the quadratic form with respect to ς. The terms involving the nonlinear function $F(\varsigma)$ can be linked with an upper bound using (28)

$$-2\eta\varsigma^T[(\hat{C} + \hat{\rho})\Xi L_1 \otimes PB]F(\varsigma) \leq -2\eta\sum_{i=1}^{M}(\hat{c}_i + \hat{\rho}_i)\varphi_i\left\|B^T P\varsigma_i\right\|\sum_{k=M+1}^{N}a_{ik} \quad \text{and} \tag{46}$$

$$-2\mu\varsigma^T[(\hat{C} + \hat{\rho})\Xi L_2 \otimes PB]F(\xi) \leq 2\mu\sum_{i=1}^{M}(\hat{c}_i + \hat{\rho}_i)\varphi_i\left\|B^T P\varsigma_i\right\|\sum_{k=M+1}^{N}a_{ik}. \tag{47}$$

Since the leaders have already achieved the formation (in Part I) specified by h_E, the following relation holds

$$x_E - h_E - \mathbf{1}_{N-M} \otimes x_{N+1} = 0 \tag{48}$$

which is equivalent to

$$(I_{N-M} \otimes I_n)(x_E - h_E - \mathbf{1}_{N-M} \otimes x_{N+1}) = 0. \tag{49}$$

Premultiplying both sides of (49) by $(C + \rho)\, \Xi L_2 L_3 \otimes PBK_2$, we have

$$[(C + \rho)\, \Xi L_2 L_3 \otimes PBK_2]\, (x_E - h_E - \mathbf{1}_{N-M} \otimes x_{N+1}) = 0. \tag{50}$$

Substituting (46), (47) and (50) into (45), we derive a simplified expression of $\dot{V}_2$ as noted below

$$\begin{aligned} \dot{V}_2 \leq \varsigma^T \left[(\hat{C} + \hat{\rho})\Xi \otimes \left(P(A + BK_1) + (A + BK_1)^T P + \Gamma\right) - \left(\lambda_1^{\min}(\hat{C} + \hat{\rho})^2 + \beta\Xi\right) \otimes \Gamma\right] \varsigma \\ - 2(\eta - \mu) \sum_{i=1}^{M} (\hat{c}_i + \hat{\rho}_i)\varphi_i \left\| B^T P \varsigma_i \right\| \sum_{k=M+1}^{N} a_{ik}. \end{aligned} \tag{51}$$

Now applying the property $X^2 + Y^2 \geq 2XY$ of positive definite matrices,[38] we obtain the following implication

$$-\varsigma^T \left[(\lambda_1^{\min}(\hat{C} + \hat{\rho})^2 + \beta\Xi) \otimes \Gamma\right] \varsigma \leq -2\varsigma^T \left[\sqrt{\lambda_1^{\min}\beta\Xi}(\hat{C} + \hat{\rho}) \otimes \Gamma\right] \varsigma. \tag{52}$$

Inequality (51) can be simplified as

$$\dot{V}_2 \leq \varsigma^T \left[(\hat{C} + \hat{\rho})\Xi \otimes \left(P(A + BK_1) + (A + BK_1)^T P - \Gamma\right)\right] \varsigma \tag{53}$$

by plugging (52) and selecting $\beta \geq \frac{\max_{i \in F} \varphi_i}{\lambda_1^{\min}}$ and $\eta \geq \mu$. Then defining a change of variable $\Upsilon = \left(\sqrt{(\hat{C} + \hat{\rho})\Xi} \otimes I\right) \varsigma$ and plugging it into (53), we have

$$\dot{V}_2 \leq \Upsilon^T \left[I_M \otimes \left(P(A + BK_1) + (A + BK_1)^T P - PBR^{-1}B^T P\right)\right] \Upsilon \tag{54}$$

which implies $\dot{V}_2 \leq 0$ using the ARE given in (19) and $\dot{V}_2 = 0$ only when $\Upsilon = 0$. Now, invoking LaSalle's invariance principle,[37] it can ensured that the containment error dynamics (40) is asymptotically stable which ultimately implies

$$\lim_{t \to \infty} \varsigma(t) = 0. \tag{55}$$

The above analysis proves that the containment error asymptotically goes to zero which in turn ensures that the followers will asymptotically converge into the convex hull spanned by the leaders. Combining Parts I and II, it can be concluded that the swarm system (1) satisfying Assumptions 1 to 4 accomplishes two-layer time-varying formation-containment tracking by applying the proposed distributed FCC protocol (6) and (7). This completes the proof. ∎

While analyzing the two-layer formation-containment problem and deriving the FCC protocol in Theorem 1, we observe a number of significant aspects which we will describe in the following remarks.

Remark 2. The formation feasibility condition (18) imposed in Theorem 1 is a common restriction in the consensus-based time-varying formation control literature.[2,30,39] This criteria needs to be checked a priori to confirm whether a desired formation shape, specified by h_E, is possible to be achieved by the leaders. In this regard, the gain matrix K_1 plays a major role in selecting the formation reference h_E as K_1 is the only parameter in the formation feasibility criteria (18) that can be freely adjusted. If it fails then the formation shape needs to be changed. In case of static formation, it is easier to find K_1 for given (A, B) of the leaders, but it may not be straightforward in case of a time-varying formation

to find an appropriate K_1 matrix to satisfy (18). In particular, it depends on the experience of a designer. However, in many practical applications, for example, in robotic applications employing nonholonomic mobile robots, the nonlinear dynamics of a robot can be feedback linearized into single or double integrator dynamics and then, it becomes much easier to find an appropriate K_1 matrix that can satisfy the formation feasibility criteria (18) for a particular choice of h_E. In this article, we have considered two case studies to address the issue of finding K_1 for a given leader's dynamics and a desired formation shape.

Remark 3. The nonlinear function $f(\cdot)$, defined in (20), is included in the proposed FCC protocols (6) and (7) to handle the time-varying dynamics of the virtual leader. By contrast to most of the existing results in the formation-containment literature, the present work does not presume the virtual leader to be an autonomous system; it may have a separate control (either reference or disturbance) input (u_{N+1}). But, the nonlinear function $f(\cdot)$ makes the FCC action *discontinuous*, which may produce "chattering effect" due to frequent "zero-crossing" and causes severe performance degradation. In order to avoid the chattering phenomenon in practical applications, the boundary layer technique proposed in Reference 9 can be exploited which redefines the nonlinear function $f(\cdot)$ to make the control action *continuous* by removing the zero-crossing criteria. Although in this method, the formation tracking or containment errors cannot be made exactly zero but can be made infinitesimally small, which is sufficient to achieve satisfactory performance and most importantly, this technique minimizes the chattering effect.

Remark 4. By contrast to the developments reported in Reference 30, where only formation-containment stabilization problem is addressed, the proposed distributed and adaptive control protocol can be used to deal with formation tracking and containment problems. Moreover, explicit computation of the smallest positive eigenvalue of the graph Laplacian matrix is avoided by using the distributed adaptive control scheme, where the agents use only relative state information of the neighbors and hence, global information about the entire graph is not required. This feature renders the proposed FCC scheme *reconfigurable* in case of communication topology changes and *scalable* for large-scale networked systems. Note further that the proposed two-layer formation-containment problem reduces to the standard "consensus problem" when $h_i = 0\ \forall i \in \{M+1, \dots, N\}$, $u_{N+1}(t) = 0$, and $M = 0$, such that the results discussed in Reference 33 can be viewed as a special case of the result of this article.

Below, we provide a set of guidelines for the control practitioners to implement the proposed distributed two-layer FCC scheme in practical applications.

Algorithm 1. Procedure to design a distributed control scheme for two-layer formation-containment problem

for each agent $i \in \{1, \dots, N\}$ **do**
  design a two-layer communication graph that satisfies Assumptions 1-4;
  fix the desired formation reference h_E for leaders;
  choose an appropriate feedback gain K_1 to widen the set of feasible formation;
  if formation feasibility condition (18) is satisfied **then**
    compute controller parameters $K_2 = -R^{-1}B^TP$ and $\Gamma = PBR^{-1}B^TP$ by solving ARE (19) for given $Q < 0$ and $R > 0$;
    design the smooth functions $\hat{\rho}_i$ and ρ_i as described in Theorem 1;
    choose positive constants η and μ according to (17) for a given $\sigma > 0$;
    construct the nonlinear function $f(.)$ according to (20);
    construct the distributed formation-containment control (FCC) protocol given in (6) and (7);
  else
    back to Step 4;
  end if
end for

In the proposed FCC scheme as derived in Theorem 1, the states of the followers converge into the convex hull spanned by the states of the leaders. However, it doesn't explicitly mention that whether the positions of the followers in a convex hull can also be controlled. In this context, the following theorem expands Theorem 1 to show an explicit relationship among the states of followers $x_i(t)$, $i \in F$, the time-varying formation of the leaders $h_i(t)$, $i \in E$, and the trajectory of the virtual leader $x_{N+1}(t)$.

Theorem 2. *Suppose the assumptions of Theorem 1 hold and the swarm system (1) achieves formation-containment by applying the distributed FCC protocol (6) and (7). The states of followers satisfy the following relationship*

$$\lim_{t\to\infty}\left(x_i(t)-\sum_{j=M+1}^{N} l_{ij}h_j(t)-x_{N+1}(t)\right)=0 \quad \forall i\in F, \tag{56}$$

where l_{ij} denotes the entries of $-L_1^{-1}L_2$.

Proof. If the assumptions of Theorem 1 are satisfied, the formation-containment of swarm system given in (1) is accomplished by applying the adaptive control laws (7) and (6). From the proof of Theorem 1, it can be readily observed that if (39) and (55) hold simultaneously, then we have

$$\lim_{t\to\infty}\left[x_F(t)-(-L_1^{-1}L_2\otimes I_n)(h_E(t)+\mathbf{1}_{N-M}\otimes x_{N+1}(t))\right]=0 \tag{57}$$

from (13) and (15). Subsequently, it follows from Lemma 2 that

$$-L_1^{-1}L_2\mathbf{1}_{N-M}=\mathbf{1}_M. \tag{58}$$

Substituting (58) into (57), we obtain

$$\lim_{t\to\infty}\left[x_F(t)-(-L_1^{-1}L_2\otimes I_n)h_E(t)-\mathbf{1}_M\otimes x_{N+1}(t))\right]=0 \tag{59}$$

which is equivalent to (56) $\forall i\in F$. This completes the proof. ∎

Theorem 2 reveals that the states of the followers are jointly determined by the communication graph, the time-varying formation of the leaders, and the formation reference. According to (56), it can be shown that the states of the followers will also give rise to a time-varying formation determined by the convex combination of the formation h_E of the leaders with respect to the formation reference x_{N+1}. Therefore, the states of the followers not only converge into the convex hull spanned by the leaders, but also maintain a time-varying formation inside the convex hull.

4 | SIMULATION CASE STUDY WITH NETWORKED ARTIFICIAL SATELLITES

In this section, a simulation case study is presented to illustrate the effectiveness of the FCC scheme developed in the previous section. Consider a network of twelve satellites and the associated communication topology is shown in Figure 1 where it is assumed that the weights of the links vary in the range [0, 1]. Figure 1 portrays that the first layer consists of six satellites considered as leaders (7-12) while the second layer contains rest six satellites which act as followers (1 to 6). The virtual target (labeled with 13) generates the tracking reference to be tracked by the leaders' formation. The dynamics of each satellite can be described by (1) with

$$A=\begin{bmatrix}0&1&0\\0&0&1\\-1&-2&-3\end{bmatrix} \quad \text{and} \quad B=\begin{bmatrix}0\\0\\1\end{bmatrix}.$$

In this case study, the virtual leader is governed by (2) with the control input $u_{N+1}=0$. Note that $u_{N+1}=0$ has been made zero only for simplicity of the pictorial representation of the simulation results. The control objective of this theoretical case study is to let the assembly of six leader satellites maintain a circular time-varying formation having hexagonal shape and keep rotating around a specific target or reference generated by the virtual leader. Then the positions of the six followers are required to converge into the convex hull spanned by the leaders. The time-varying circular formation

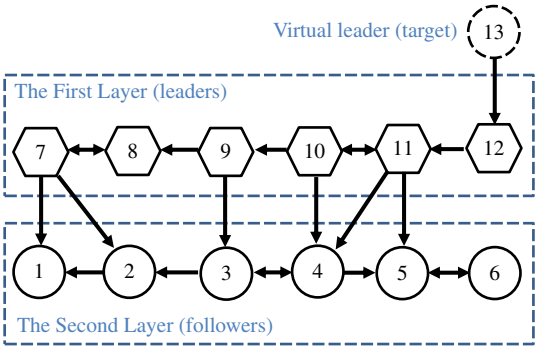

FIGURE 1 A two-layer directed communication topology among twelve satellites is shown of which six are considered as leaders (labeled with 7-12) while the rest six are the followers (labeled with 1-6) and the virtual leader (or the target) is labeled with 13 [Colour figure can be viewed at wileyonlinelibrary.com]

of the leaders is specified by

$$h_i(t) = \begin{bmatrix} 15\sin(t + \frac{(i-7)\pi}{3}) \\ 15\cos(t + \frac{(i-7)\pi}{3}) \\ -15\sin(t + \frac{(i-7)\pi}{3}) \end{bmatrix} \quad \forall i \in \{7, 8, \dots, 12\}\,.$$

$K_1 = \begin{bmatrix} -3 & 1 & -1 \end{bmatrix}$ is chosen such that the formation tracking feasibility condition (19) in Theorem 1 is satisfied with this desired $h_i(t)$ $\forall i \in \{7, 8, \dots, 12\}$. Thus, if the predefined time-varying formation $h_i(t)$ is achieved, the six leaders will be placed at the six vertices of a parallel hexagon and keep rotating around the reference signal with an angular velocity of 1 rad/s. The followers will also converge into the parallel hexagon formed by the leaders.

Now choosing $Q = \begin{bmatrix} 1 & 0 & 0 \\ 0 & 1 & 0 \\ 0 & 0 & 1 \end{bmatrix}$, $R = 0.1$ and $\eta = \mu = 0.2$ for a given $\sigma = 0$, the controller gain matrices are calculated as

$$K_2 = \begin{bmatrix} -2.3166 & -4.5719 & -2.3051 \end{bmatrix} \quad \text{and} \quad \Gamma = \begin{bmatrix} 0.5368 & 1.0593 & 0.5341 \\ 1.0591 & 2.0903 & 1.0539 \\ 0.5340 & 1.0538 & 0.5313 \end{bmatrix}$$

following Algorithm 1. Let the initial values of the coupling weights be $\hat{c}_i(0) = 0$ and $c_i(0) = 0$ for all $i \in \{1, 2, \dots, 12\}$ and the initial states of each of the twelve satellites be chosen pseudorandomly with a uniform distribution in the interval $(-10, 10)$.

The spatial positions of the satellites at different time instants during the formation-containment phase are depicted in Figure 2A-D; while Figure 3 shows the desired formation reference trajectory. The figures suggest that the six leader satellites have attained a hexagonal formation (Green colored) in the 3D plane which keeps rotating around the desired target (marked by the Red star in Figure 2A-D) and the follower satellites eventually converge into this hexagonal region formed by the leaders while maintaining the same angular velocity as that of the leaders. Time variation of the coupling weights $\hat{c}_i(t)$ of the followers and $c_i(t)$ of the leaders are plotted in Figure 4 which shows that the coupling weights converge to finite steady values within finite time. 2-norms of the formation tracking error of the leaders (ς) and the containment error of the followers (ξ) are depicted in Figure 5A,B. It is now concluded that the desired time-varying formation-containment is achieved under the influence of the distributed FCC protocol as given in (6) and (7).

5 | EXPERIMENTAL VALIDATION RESULTS WITH NONHOLONOMIC MOBILE ROBOTS

In the hardware experiment, we used small-scale, autonomous mobile robots, Mona,[40] to test the feasibility of the proposed FCC scheme. Mona is a low-cost, open-source, miniature robot which has been developed for swarm robotic applications. As shown in Figure 6, Mona has two 6V low power DC geared-motors connected directly to its wheels having 32mm diameter and the robot has a circular chassis having 80mm diameter. The main processor embedded in this robot is an AVR microcontroller equipped with an external clock having 16 MHz frequency. Each robot is equipped with NRF24101 wireless transceiver module for interrobot communication. The robots are operated and controlled by

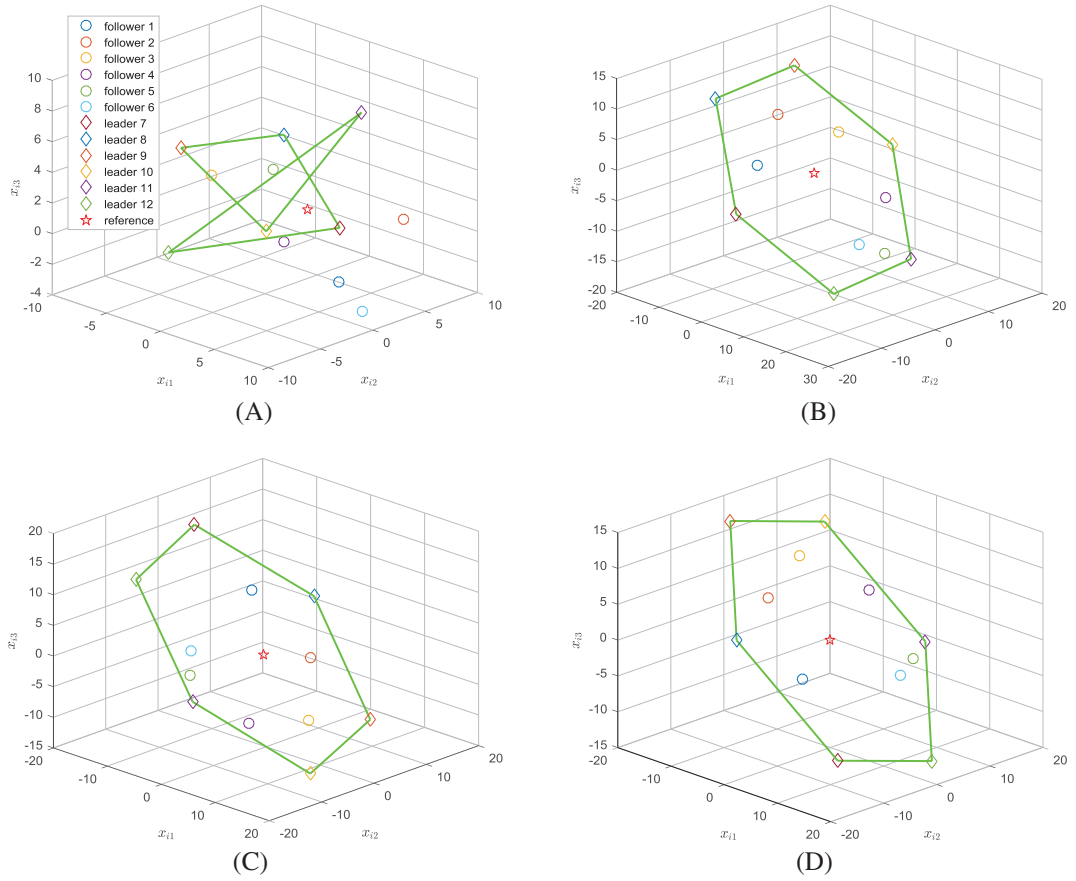

FIGURE 2 Spatial position of the satellites at the time instants: A, $t = 0$ s, B, $t = 10$ s, C, $t = 20$ s, and D, $t = 40$ s during the formation-containment course [Colour figure can be viewed at wileyonlinelibrary.com]

FIGURE 3 Trajectory of the target to be tracked which is generated by the virtual leader (labeled as 13 in Figure 1) [Colour figure can be viewed at wileyonlinelibrary.com]

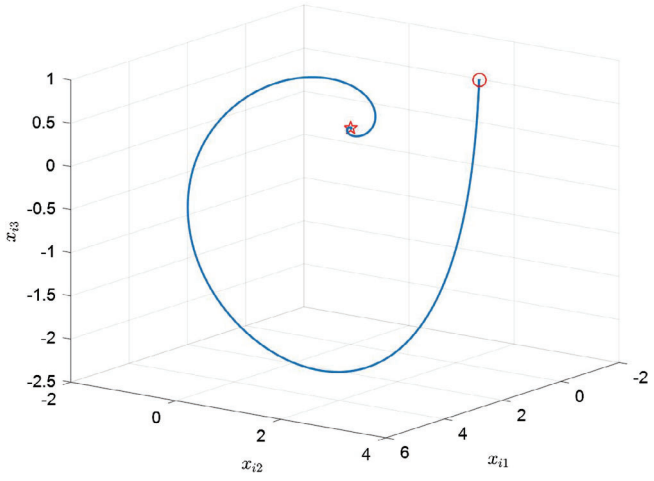

Arduino Mini/Pro microcontroller boards which are programmed by using the existing open-source software modules. The experimental platform includes a $1.2m \times 1.2m$ blue arena and a digital camera connected to a host PC which operates the entire tracking system. The position tracking system used in this experiment is an open-source multirobot localization platform.[41] The tracking system is not only capable of following a robot's position but also capable of measuring its velocity and detecting its orientations by identifying the unique circular tags attached on top of the robots. The state information is transmitted to the computer via the ROS communication framework and then the relative state information is sent to the corresponding robot using RF transceiver module.

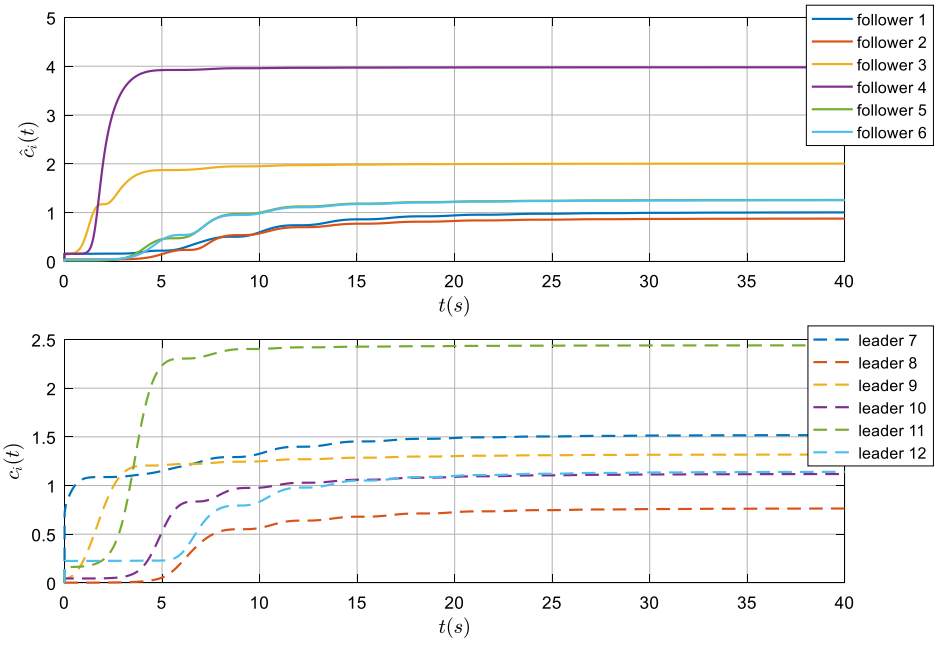

FIGURE 4 Time evolvement of the coupling weights $\hat{c}_i(t)$ of the followers and $c_i(t)$ of the leaders [Colour figure can be viewed at wileyonlinelibrary.com]

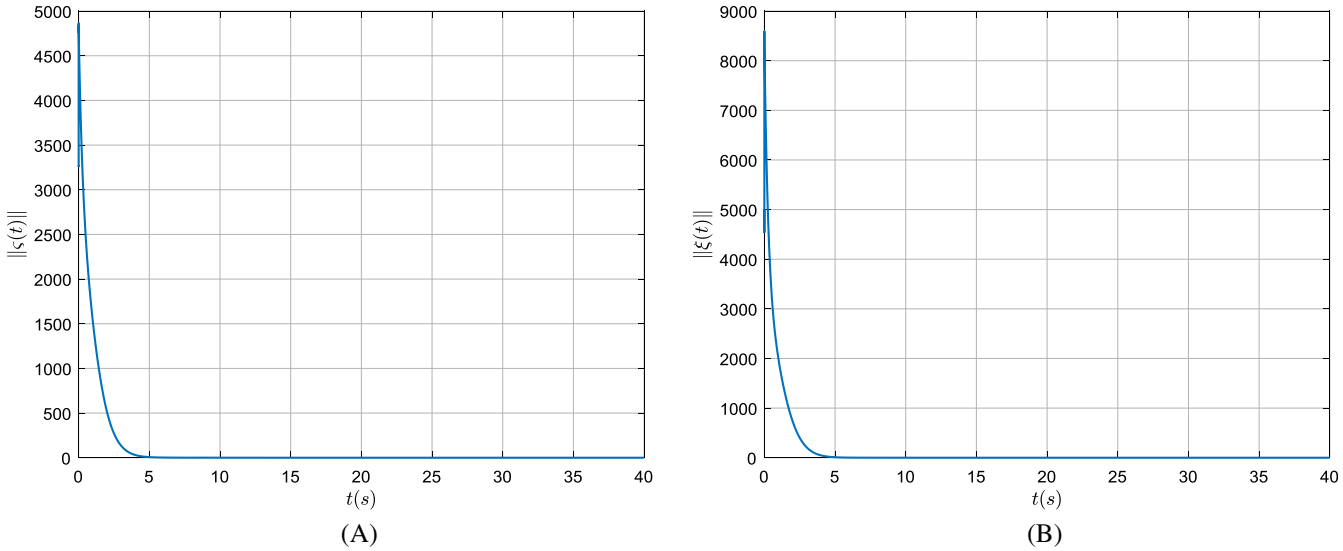

FIGURE 5 Tine variation of the 2-norm of A, containment error vector ς and B, formation error vector ξ [Colour figure can be viewed at wileyonlinelibrary.com]

In the experiment, six nonholonomic mobile robots (Mona) were considered to perform a formation-containment activity. Each mobile robot can be described by the following set of dynamic equations in terms of the global coordinates

$$\begin{cases} \dot{x}_{xi} = v_i \cos\theta_i \\ \dot{x}_{yi} = v_i \sin\theta_i \\ \dot{\theta}_i = \omega_i \end{cases} \qquad \forall i \in \{1, \ldots, 6\}$$

where x_{xi} and x_{yi} together represent the position of the *ith* robot in the $X-Y$ plane in terms of the Cartesian coordinate, θ_i is the angle between the heading direction and the X axis, v_i denotes the linear velocity and ω_i represents the angular velocity. For each mobile robot, we introduce a new control input q_i such that

$$\dot{v}_i = q_i \quad \forall i \in \{1, \ldots, 6\}.$$

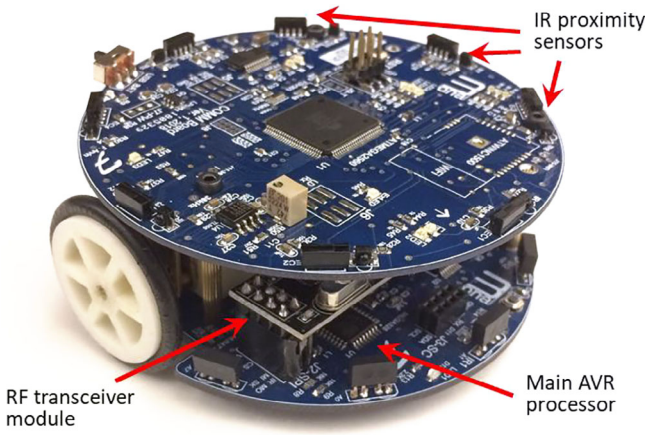

FIGURE 6 The autonomous mobile robot, Mona,[40] used in the hardware experiment [Colour figure can be viewed at wileyonlinelibrary.com]

Define $v_{xi} = v_i \cos\theta_i$ and $v_{yi} = v_i \sin\theta_i$ which represent, respectively, the X-axis and Y-axis components of the linear velocity v_i. Therefore, $\dot{x}_{xi} = v_{xi}$ and $\dot{x}_{yi} = v_{yi}$. Subsequently, by taking the time-derivative of v_{xi} and v_{yi} are computed as

$$\begin{bmatrix} \dot{v}_{xi} \\ \dot{v}_{yi} \end{bmatrix} = \begin{bmatrix} \cos\theta_i & -v_i \sin\theta_i \\ \sin\theta_i & v_i \cos\theta_i \end{bmatrix} \begin{bmatrix} q_i \\ \omega_i \end{bmatrix}.$$

Now a feedback linearizing control law is designed below by assuming $v_i \neq 0$

$$\begin{bmatrix} q_i \\ \omega_i \end{bmatrix} = \begin{bmatrix} \cos\theta_i & \sin\theta_i \\ -\frac{\sin\theta_i}{v_i} & -\frac{\cos\theta_i}{v_i} \end{bmatrix} \begin{bmatrix} u_{xi} \\ u_{yi} \end{bmatrix}$$

such that the nonlinear dynamics of the robots can be linearized into the form $\dot{x}_i = Ax_i + Bu_i$, as given in (1), with

$$A = \begin{bmatrix} 0 & 1 & 0 & 0 \\ 0 & 0 & 0 & 0 \\ 0 & 0 & 0 & 1 \\ 0 & 0 & 0 & 0 \end{bmatrix} \quad \text{and} \quad B = \begin{bmatrix} 0 & 0 \\ 1 & 0 \\ 0 & 0 \\ 0 & 1 \end{bmatrix}, \tag{60}$$

where $x_i = \left[x_{xi}, v_{xi}, x_{yi}, v_{yi}\right]^T$ and $u_i = \left[u_{xi}, u_{yi}\right]^T$ represent the state vector and the control input vector of the feedback linearized system, respectively.

In this experimental demonstration, the four leader robots will form a square-shaped region (ie, the convex hull) in the experimental arena and the two follower robots is expected to converge into this safe region. Figure 7 depicts the directed interaction topology among the six mobile robots. The state of the virtual leader (labeled with no. 7) is arbitrarily chosen as $[0.7, 0, 0.7, 0]^T$. The control objective of this experiment is to let the four leader robots to achieve a planar square formation, tracking the virtual target and keep surrounding the followers. The time-varying circular formation for the leader robots is specified by

$$h_i(t) = \begin{bmatrix} r\sin(\omega t + \frac{2(i-1)\pi}{4}) \\ \omega r\cos(\omega t + \frac{2(i-1)\pi}{4}) \\ r\cos(\omega t + \frac{2(i-1)\pi}{4}) \\ -\omega r\sin(\omega t + \frac{2(i-1)\pi}{4}) \end{bmatrix} \quad \forall i \in \{3, 4, 5, 6\}$$

where $r = 0.3$ m and $\omega = 0.1$ rad/s denote, respectively, the radius and angular velocity of the desired time-varying formation. It can be verified that the formation tracking feasibility condition (18) of Theorem 1 is satisfied in the present scenario and hence, when the predefined time-varying formation $h_i(t)$ is achieved, the leaders will automatically be placed at the four vertices of a square. After attaining the desired formation, the assembly of the leader robots keeps on rotating around the tracking reference with a constant angular velocity of 0.1 rad/s and two follower robots will eventually converge into this area.

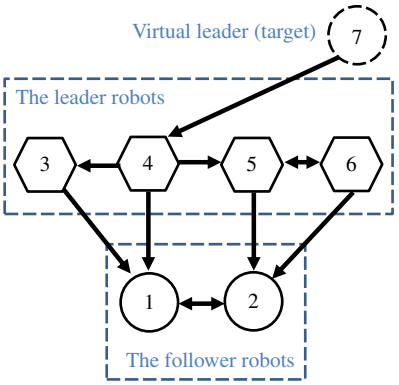

FIGURE 7 The directed communication topology among the robots considered in the hardware experiment [Colour figure can be viewed at wileyonlinelibrary.com]

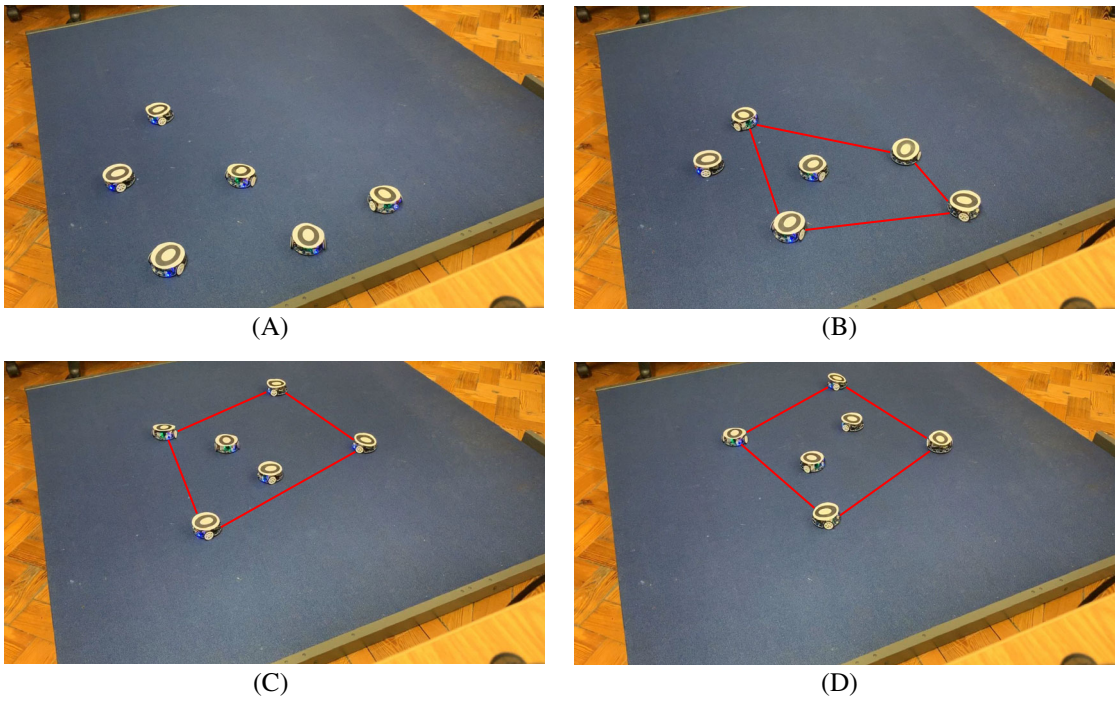

FIGURE 8 Progress of the formation-containment mission being achieved by a team of six mobile robots in real-time hardware experiment. A, Initial orientation of the robots at $t = 0$ s; B, At $t = 20$ s: leader robots are about to attain the desired square formation; C, At $t = 40$ s: leaders have already achieved the formation and two follower robots have also converged into the area spanned by the leaders; D, At $t = 80$ s: the whole assembly of the leaders has moved toward the center of the arena following the location of the given target along with the followers being surrounded by them—mission accomplished [Colour figure can be viewed at wileyonlinelibrary.com]

Figure 8A-D presents the hardware experiment results on achieving the formation-containment by a team of six non-holonomic mobile robots (Mona) on a planar surface. Figure 8A shows the initial orientation (at $t = 0$ s) of the robots on the arena. Figure 8B depicts the progress of the mission at $t = 20$ s from which it is apparent that the four leader robots are moving in the right track to attain the expected square formation and subsequently, Figure 8C reveals that the leader robots have truly achieved the desired square formation (at $t = 40$ s) and the two follower robots have also converged into the area spanned by the leaders. Finally, Figure 8D portrays that the assembly of the leaders has moved toward the center of the arena in order to track the position of the given target without disturbing the formation and the followers have also moved accordingly being surrounded by the leaders. This then concludes that the formation-containment mission has been achieved successfully under the application of the proposed distributed FCC scheme. Figure 9 complements the hardware experiment result presented in Figure 8A-D by plotting the position trajectories of all six robots in the XY plane during the course of achieving the formation tracking and containment in the hardware experiment. Figure 9 traces the movement of the robots staring from the initial positions until they converge at the desired locations to attain the leaders' formation around the given target (marked by the Red star) and the followers' containment within the area spanned by the positions of the leader robots. Finally, time evolvement of the 2-norms of the formation tracking error $\xi_i(t)$

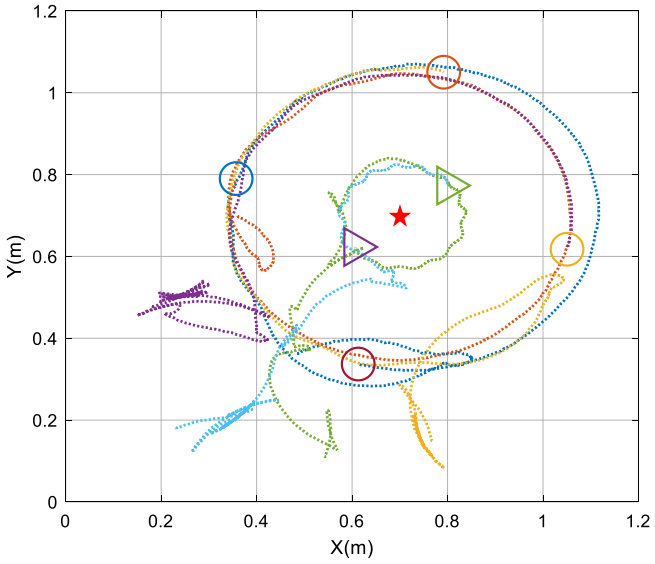

FIGURE 9 Position trajectories of the robots in the *XY* plane during the course of achieving formation tracking and containment in the hardware experiment under the application of the proposed FCC protocol. In this figure, the circles represent the leaders, the triangles denote the followers and the star indicates the target to be tracked. FCC, formation-containment control [Colour figure can be viewed at wileyonlinelibrary.com]

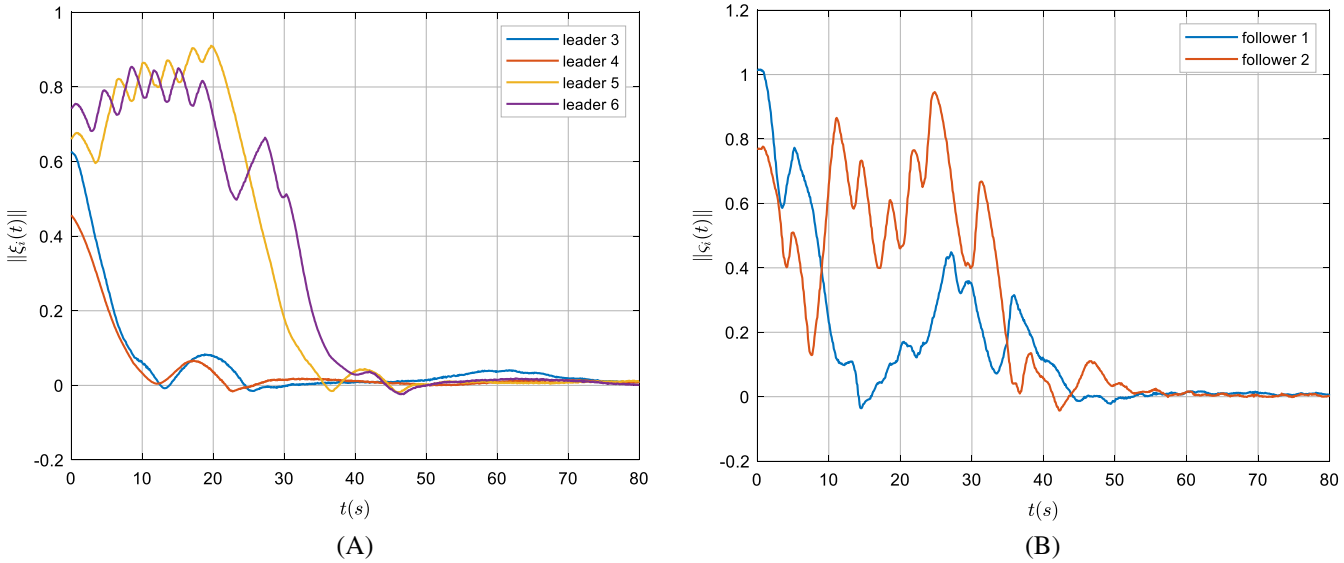

FIGURE 10 Time variation of the 2-norms of A, formation tracking error $\xi_i(t)$ of the leaders and B, containment error $\varsigma_i(t)$ of the followers [Colour figure can be viewed at wileyonlinelibrary.com]

of four leaders and the containment error $\varsigma_i(t)$ of two followers are shown in Figure 10A,B. The figures reveal that both the formation tracking and containment errors die down to zero within 80 seconds which is in agreement with the fact that the experiment also took 80 seconds to accomplish the mission as reflected in Figure 8D. It can hence be ascertained that both formation tracking and containment have been achieved by the team of six mobile robots under the influence of the proposed distributed FCC scheme.

Even though we have used lab-based experimental set-up, small-scale robots and open source software modules, but the experimental results reflect usefulness of the proposed scheme in finding potential applications in robotics. High precision performance is also possible to be achieved by the proposed scheme with improvised camera tracking system, high-end embedded microcontrollers and advanced robots.

6 | CONCLUSIONS

In this article, a formation-containment problem for linear swarm systems connected via directed graphs is investigated. A two-layer distributed FCC scheme is proposed for LTI swarm systems that can be decomposed into leaders' formation

layer and the followers' containment layer. The proposed FCC protocols are adaptive and constructed based on relative state information of the agents which enables the scheme to work without using global information about the interaction topology. Theoretical basis of the proposed scheme has been established using the Lyapunov stability framework and the control parameters are chosen via solving an algebraic Riccati equation. It is also proved that the states of followers not only converge into the convex hull spanned by the leaders but also maintain certain formation determined by the leaders and the virtual agent. An algorithm is also written for the control practitioners to identify the design steps to implement the proposed scheme in practice. A simulation case study has been conducted on achieving the formation-containment tasks of networked satellites to highlight the usefulness of the proposed FCC scheme and finally, experimental validation results involving networked mobile robots are also included to show the feasibility of the proposed scheme in real-time implementation. In future scope, the present FCC scheme may be extended to consider the effects of time delays and nonlinear dynamics of the robotic systems. Furthermore, robust distributed controller design techniques can also be explored by utilizing the ideas of References 42-45.

ACKNOWLEDGEMENTS

This work was supported by the Engineering and Physical Sciences Research Council (EPSRC) [grant number EP/R008876/1]. All research data supporting this publication are directly available within this publication.

ORCID

Junyan Hu https://orcid.org/0000-0001-7409-3885

REFERENCES

1. Wang X, Yadav V, Balakrishnan SN. Cooperative UAV formation flying with obstacle/collision avoidance. *IEEE Trans Control Syst Technol*. 2007;15(4):672-679.
2. Hu J, Lanzon A. An innovative tri-rotor drone and associated distributed aerial drone swarm control. *Robot Auton Syst*. 2018;103:162-174.
3. Ou M, Du H, Li S. Finite-time formation control of multiple nonholonomic mobile robots. *Int J Robust Nonlinear Control*. 2014;24(1):140-165.
4. Hu J, Lanzon A. Distributed finite-time consensus control for heterogeneous battery energy storage systems in droop-controlled microgrids. *IEEE Trans Smart Grid*. 2019;10(5):4751-4761.
5. Hu J, Bhowmick P, Arvin F, Lanzon A, Lennox B. Cooperative control of heterogeneous connected vehicle platoons: an adaptive leader-following approach. *IEEE Robot Autom Lett*. 2020;5(2):977-984.
6. Wang J, Lanzon A, Petersen IR. Robust output feedback consensus for networked negative-imaginary systems. *IEEE Trans Autom Control*. 2015;60(9):2547-2552.
7. Wang J, Lanzon A, Petersen IR. Robust cooperative control of multiple heterogeneous negative-imaginary systems. *Automatica*. 2015;61:64-72.
8. Yang C, Chen F, Xiang L, Lan W. Distributed rendezvous and tracking for multiple unicycles with heterogeneous input disturbances. *Int J Robust Nonlinear Control*. 2017;27(9):1589-1606.
9. Zhongkui L, Duan Z, Ren W, Feng G. Containment control of linear multi-agent systems with multiple leaders of bounded inputs using distributed continuous controllers. *Int J Robust Nonlinear Control*. 2015;25(13):2101-2121.
10. Klotz JR, Cheng T-H, Dixon WE. Robust containment control in a leader–follower network of uncertain Euler–Lagrange systems. *Int J Robust Nonlinear Control*. 2016;26(17):3791-3805.
11. Wang J, Xin M. Integrated optimal formation control of multiple unmanned aerial vehicles. *IEEE Trans Control Syst Technol*. 2013;21(5):1731-1744.
12. Hu J, Lanzon A. Cooperative control of innovative tri-rotor drones using robust feedback linearization. Paper presented at: Proceedings of 12th UKACC International Conference on Control; 2018;347-352.
13. Ren W. Consensus strategies for cooperative control of vehicle formations. *IET Control Theory Appl*. 2007;1(2):505-512.
14. Hu J, Lanzon A. Cooperative adaptive time-varying formation tracking for multi-agent systems with LQR performance index and switching directed topologies. Paper presented at: Proceedings of 57th IEEE Conference on Decision and Control; 2018;5102-5107.
15. Xiao F, Wang L, Chen J, Gao Y. Finite-time formation control for multi-agent systems. *Automatica*. 2009;45(11):2605-2611.
16. Du H, Li S, Lin X. Finite-time formation control of multiagent systems via dynamic output feedback. *Int J Robust Nonlinear Control*. 2013;23(14):1609-1628.
17. Fax JA, Murray RM. Information flow and cooperative control of vehicle formations. *IEEE Trans Autom Control*. 2004;49(9):1465-1476.
18. Porfiri M, Roberson DG, Stilwell DJ. Tracking and formation control of multiple autonomous agents: a two-level consensus approach. *Automatica*. 2007;43(8):1318-1328.
19. Hu J, Bhowmick P, Lanzon A. Distributed adaptive time-varying group formation tracking for multi-agent systems with multiple leaders on directed graphs. *IEEE Trans Control Netw Syst*. 2020;7(1):140-150.
20. Turpin M, Michael N, Kumar V. Decentralized formation control with variable shapes for aerial robots. Paper presented at: Proceeding of IEEE International Conference on Robotics and Automation, Vol. 1; 2012;23-30.

21. Li Z, Ren W, Liu X, Fu M. Distributed containment control of multi-agent systems with general linear dynamics in the presence of multiple leaders. *Int J Robust Nonlinear Control*. 2013;23(5):534-547.
22. Cao Y, Ren W, Egerstedt M. Distributed containment control with multiple stationary or dynamic leaders in fixed and switching directed networks. *Automatica*. 2012;48(8):1586-1597.
23. Cao Y, Stuart D, Ren W, Meng Z. Distributed containment control for multiple autonomous vehicles with double-integrator dynamics: algorithms and experiments. *IEEE Trans Control Syst Technol*. 2011;19(4):929-938.
24. Mei J, Ren W, Ma G. Distributed containment control for Lagrangian networks with parametric uncertainties under a directed graph. *Automatica*. 2012;48(4):653-659.
25. Chen L-M, Li C-J, Mei J, Ma G-F. Adaptive cooperative formation-containment control for networked Euler–Lagrange systems without using relative velocity information. *IET Control Theory Appl*. 2017;11(9):1450-1458.
26. Li C, Chen L, Guo Y, Ma G. Formation–containment control for networked Euler–Lagrange systems with input saturation. *Nonlinear Dyn*. 2018;91(2):1307-1320.
27. Chen L, Li C, Xiao B, Guo Y. Formation-containment control of networked Euler–Lagrange systems: an event-triggered framework. *ISA Trans*. 2019;86:87-97.
28. Liu H, Cheng L, Tan M, Hou Z, Cao Z, Wang M. Containment control with multiple interacting leaders under switching topologies. Paper presented at: Proceedings of 32nd Chinese Control Conference, Vol. 1; 2013;7093-7098.
29. Zheng B, Mu X. Formation-containment control of second-order multi-agent systems with only sampled position data. *Int J Syst Sci*. 2016;47(15):3609-3618.
30. Dong X, Shi Z, Lu G, Zhong Y. Formation-containment analysis and design for high-order linear time-invariant swarm systems. *Int J Robust Nonlinear Control*. 2015;25(17):3439-3456.
31. Wang Y-W, Liu X-K, Xiao J-W, Lin X. Output formation-containment of coupled heterogeneous linear systems under intermittent communication. *J Franklin Inst*. 2017;354(1):392-414.
32. Zuo S, Song Y, Lewis FL, Davoudi A. Time-varying output formation-containment of general linear homogeneous and heterogeneous multi-agent systems. *IEEE Trans Control Netw Syst*. 2019;6(2):537-548. https://doi.org/10.1109/TCNS.2018.2847039.
33. Lv Y, Li Z, Duan Z, Feng G. Novel distributed robust adaptive consensus protocols for linear multi-agent systems with directed graphs and external disturbances. *Int J Control*. 2017;90(2):137-147.
34. Li Z, Duan Z. *Cooperative Control of Multi-Agent Systems: A Consensus Region Approach*. 1st ed. Boca Raton, FL: CRC Press; 2017.
35. Zhang H, Lewis FL, Qu Z. Lyapunov, adaptive, and optimal design techniques for cooperative systems on directed communication graphs. *IEEE Trans Ind Electron*. 2012;59(7):3026-3041.
36. Meng Z, Ren W, You Z. Distributed finite-time attitude containment control for multiple rigid bodies. *Automatica*. 2010;46(12):2092-2099.
37. Khalil HK. *Nonlinear Systems*. 3rd ed. Upper Saddle River, NJ: Prentice-Hall; 2002.
38. Bernstein DS. *Matrix Mathematics: Theory, Facts, and Formulas with Application to Linear Systems Theory*. Princeton, NJ: Princeton University Press; 2005.
39. Dong X, Li Q, Zhao Q, Ren Z. Time-varying group formation analysis and design for general linear multi-agent systems with directed topologies. *Int J Robust Nonlinear Control*. 2017;27(9):1640-1652.
40. Arvin F, Espinosa J, Bird B, West A, Watson S, Lennox B. Mona: an affordable open-source mobile robot for education and research. *J Intell Robot Syst*. 2019;94:761-775.
41. Krajník T, Nitsche M, Faigl J, et al. A practical multirobot localization system. *J Intell Robot Syst*. 2014;76(3-4):539-562.
42. Lanzon A, Chen H-J. Feedback stability of negative imaginary systems. *IEEE Trans Autom Control*. 2017;62(11):5620-5633.
43. Song Z, Lanzon A, Patra S, Petersen IR. Robust performance analysis for uncertain negative-imaginary systems. *Int J Robust Nonlinear Control*. 2012;22(3):262-281.
44. Bhowmick P, Patra S. On LTI output strictly negative-imaginary systems. *Syst Control Lett*. 2017;100:32-42.
45. Bhowmick P, Patra S. On decentralized integral controllability of stable negative-imaginary systems and some related extensions. *Automatica*. 2018;94:443-451.

SUPPORTING INFORMATION

Additional supporting information may be found online in the Supporting Information section at the end of this article.

How to cite this article: Hu J, Bhowmick P, Lanzon A. Two-layer distributed formation-containment control strategy for linear swarm systems: Algorithm and experiments. *Int J Robust Nonlinear Control*. 2020;30:6433–6453. https://doi.org/10.1002/rnc.5105